Cell Reports

Article

Leishmania Lipophosphoglycan Triggers Caspase-11 and the Non-canonical Activation of the NLRP3 Inflammasome

Graphical Abstract

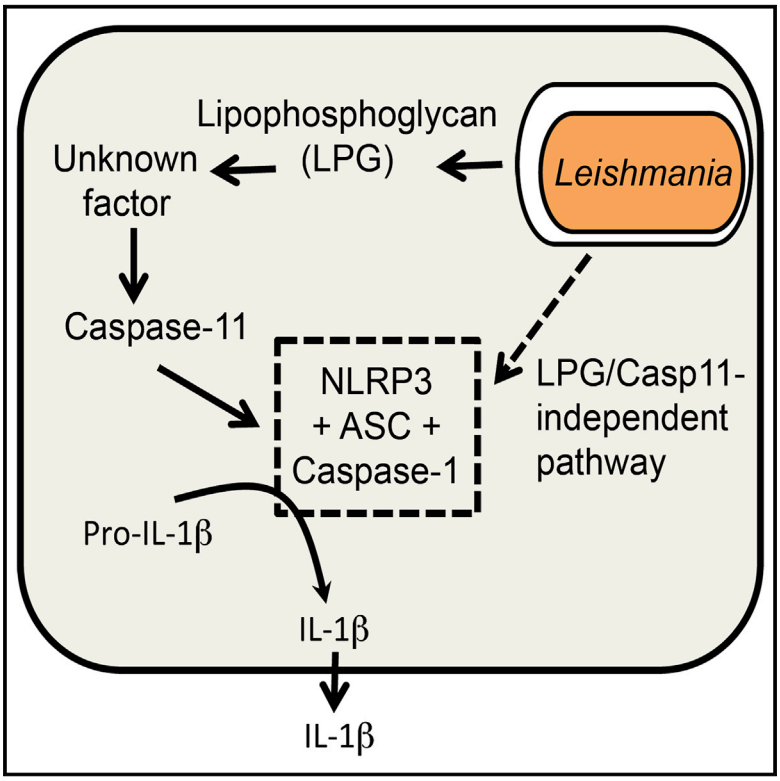

Highlights

- *Leishmania* infection triggers the non-canonical activation of the NLRP3 inflammasome
- *Leishmania* lipophosphoglycan (LPG) triggers caspase-11 activation
- LPG-deficient *Leishmania* shows impaired caspase-11 and caspase-1 activation
- Caspase-11 is important for restriction of *Leishmania* infection in macrophages and *in vivo*

Authors

Renan V.H. de Carvalho, Warrison A. Andrade, Djalma S. Lima-Junior, ..., Stephen M. Beverley, Feng Shao, Dario S. Zamboni

Correspondence

dszamboni@fmrp.usp.br

In Brief

Activation of the NLRP3 inflammasome is critical for the outcome of leishmaniasis. De Carvalho et al. show that *Leishmania* lipophosphoglycan (LPG) triggers caspase-11 activation in macrophage cytoplasm and the non-canonical activation of NLRP3, thereby establishing the mechanisms underlying NLRP3 activation in response to *Leishmania*.

de Carvalho et al., 2019, Cell Reports *26*, 429–437
January 8, 2019
https://doi.org/10.1016/j.celrep.2018.12.047

CellPress

Cell Reports
Article

Leishmania Lipophosphoglycan Triggers Caspase-11 and the Non-canonical Activation of the NLRP3 Inflammasome

Renan V.H. de Carvalho,[1,5] Warrison A. Andrade,[1,5] Djalma S. Lima-Junior,[1] Marisa Dilucca,[1] Caroline V. de Oliveira,[1] Kun Wang,[2] Paula M. Nogueira,[3] Jeronimo N. Rugani,[3] Rodrigo P. Soares,[3] Stephen M. Beverley,[4] Feng Shao,[2] and Dario S. Zamboni[1,6,*]

[1]Departamento de Biologia Celular e Molecular e Bioagentes Patogênicos, Faculdade de Medicina de Ribeirão Preto, Universidade de São Paulo, Ribeirão Preto, São Paulo, Brazil
[2]National Institute of Biological Sciences, Beijing, 102206, China
[3]Instituto René Rachou, Fundação Oswaldo Cruz - FIOCRUZ, Belo Horizonte, Brazil
[4]Department of Molecular Microbiology, Washington University School of Medicine, Saint Louis, MO 63110, USA
[5]These authors contributed equally
[6]Lead Contact
*Correspondence: dszamboni@fmrp.usp.br
https://doi.org/10.1016/j.celrep.2018.12.047

SUMMARY

Activation of the NLRP3 inflammasome by *Leishmania* parasites is critical for the outcome of leishmaniasis, a disease that affects millions of people worldwide. We investigate the mechanisms involved in NLRP3 activation and demonstrate that caspase-11 (CASP11) is activated in response to infection by *Leishmania* species and triggers the non-canonical activation of NLRP3. This process accounts for host resistance to infection in macrophages and *in vivo*. We identify the parasite membrane glycoconjugate lipophosphoglycan (LPG) as the molecule involved in CASP11 activation. Cytosolic delivery of LPG in macrophages triggers CASP11 activation, and infections performed with *Lpg1*$^{-/-}$ parasites reduce CASP11/NLRP3 activation. Unlike bacterial LPS, purified LPG does not activate mouse CASP11 (or human Casp4) *in vitro*, suggesting the participation of additional molecules for LPG-mediated CASP11 activation. Our data identify a parasite molecule involved in CASP11 activation, thereby establishing the mechanisms underlying inflammasome activation in response to *Leishmania* species.

INTRODUCTION

Leishmaniasis is a chronic inflammatory disease caused by the protozoan parasite of the *Leishmania* genus. The disease is widespread in tropical and subtropical areas of the globe, including Europe, Africa, Asia, and the Americas, and affects millions of people (Alvar et al., 2012). Species such as *Leishmania (Leishmania) amazonensis* and *L. (Viannia) braziliensis* induce cutaneous leishmaniasis, which manifests as a localized form of the disease and can progress to more severe forms, such as diffuse and mucocutaneous, respectively. In contrast, *L. (L.) infantum* causes a life-threatening visceral form of leishmaniasis (Chappuis et al., 2007; Reithinger et al., 2007). It is estimated that 350 million people are at risk, and more than 2 million new cases appear every year. Most infected people are asymptomatic, whereas 12 million patients have active disease, and 20,000–50,000 eventually die (Alvar et al., 2012; World Health Organization, 2010).

Leishmania spp. interact with many cell types, including neutrophils, monocytes, and macrophages, where they differentiate into amastigotes and replicate inside the parasitophorous vacuole. Innate immune receptors present in these professional phagocytes are critical for initiating an effective and protective immune response against the disease (Kaye and Scott, 2011; Zamboni and Lima-Junior, 2015). Recent studies have indicated that intracellular receptors from the family of the nucleotide-binding domain and leucine-rich repeat-containing proteins (NLRs) are critical for the outcome of leishmaniasis (Charmoy et al., 2016; Gurung et al., 2015; Lima-Junior et al., 2013, 2017). NLRP3 is the most studied NLR; it is associated with the pathogenesis of several inflammatory diseases and is also involved in the sensing and restriction of infection by several microorganisms, including bacteria and parasites (reviewed in Broz and Dixit, 2016; Zamboni and Lima-Junior, 2015). A wide variety of stimuli, such as toxins, crystals, ATP, cathepsins, and reactive oxygen species (ROS), have been shown to trigger the canonical NLRP3 inflammasome, but NLRP3 can also be activated via murine caspase-11 (CASP11; an ortholog of human Casp4 and Casp5), which recognizes bacterial lipopolysaccharide (LPS) in the cytoplasm and induces the non-canonical activation of the NLRP3 inflammasome (Hagar et al., 2013; Kayagaki et al., 2013; Shi et al., 2014).

Although LPS is the major glycolipid present in Gram-negative bacteria, lipophosphoglycan (LPG) is the major glycoconjugate present on the surface of *Leishmania* parasites (reviewed in Turco and Descoteaux, 1992). LPG has been implicated in cytokine production via Toll-like receptors (TLRs), attachment and entry into macrophages, inhibition of phagosomal maturation, protection from proteolytic damage within acidic vacuoles, and induction of neutrophil extracellular traps (reviewed in de Assis et al., 2012; Franco et al., 2012; Matte and Descoteaux, 2016).

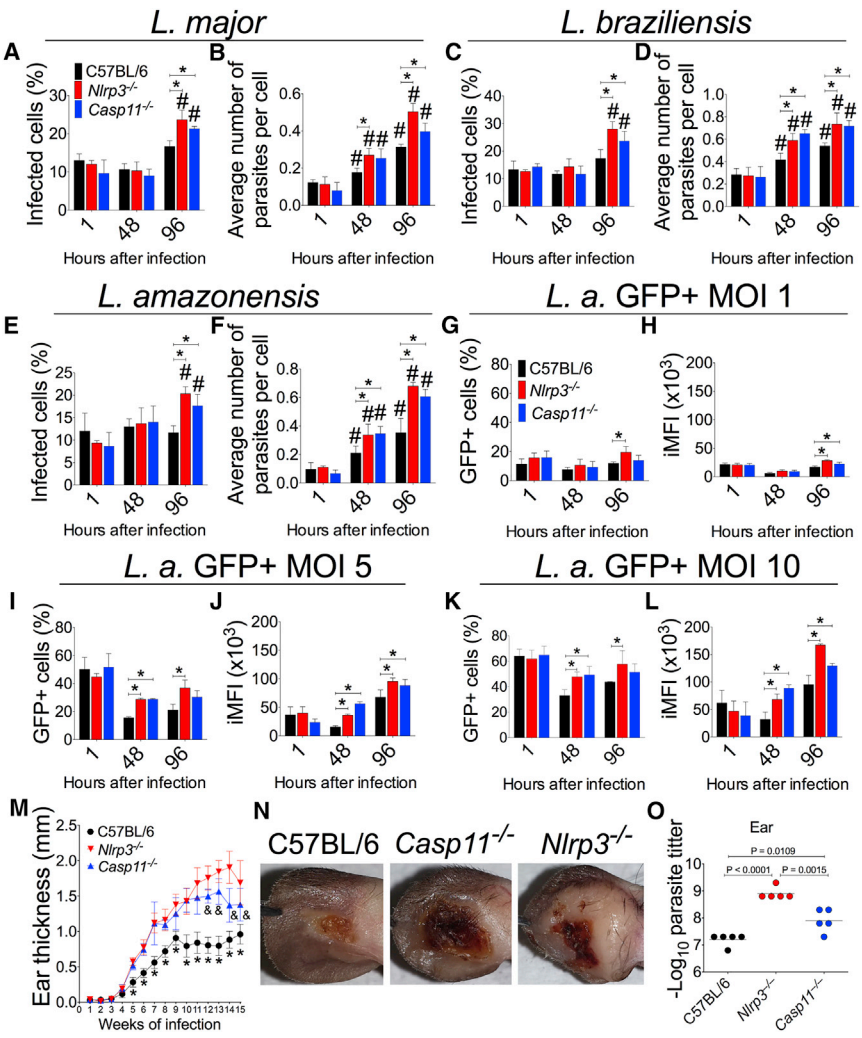

Figure 1. Caspase-11 Is Important for Controlling *Leishmania* spp. Infection *In Vitro* and *In Vivo*

(A–L) C57BL/6, *Nlrp3*$^{-/-}$, and *Casp11*$^{-/-}$ BMDMs were infected with metacyclic promastigotes from *L. major* (A and B), *L. braziliensis* (C and D), and *L. amazonensis* (E and F) at an MOI of 1 or different MOIs of stationary-phase promastigotes from *L. amazonensis*-GFP^{+} (*L.a.*-GFP^{+}) (G–L) for 1 hr, washed, and incubated for 48 and 96 hr. Cells infected with *L. amazonensis* GFP^{+} at MOI 1 (G and H), MOI 5 (I and J), or MOI 10 (K and L) were detached from plates and analyzed by FACS. The percentage of infected cells and the average number of parasites per cell were determined by Giemsa staining (A–F). In (A)–(F), pound sign indicates statistical difference of 48 or 96 hr compared with 1 hr group of the same genotype. The percentage of *L. amazonensis*-GFP^{+} cells and the integrated mean fluorescence intensity (iMFI) of GFP-expressing parasites were quantified using flow cytometry.

(M–O) C57BL/6, *Nlrp3*$^{-/-}$, and *Casp11*$^{-/-}$ mice (n = 5 mice per group) were infected with 10^3 metacyclic *L. amazonensis* promastigotes in the ear, and the ear thicknesses were followed for 15 weeks (M). Images of infected ears (N) and parasite quantification (O) at 15 weeks post-infection.

The data are represented as the mean ± SD of triplicate samples and are representative of the data obtained from three (A–F) or two (G–O) independent experiments. Statistical analysis was performed using Student's t test (A–L and O) or two-way ANOVA with Bonferroni's multiple-comparison test (M). Asterisks indicate significant differences ($p < 0.05$) between indicated groups and WT BMDMs (A–L and O), whereas asterisk and ampersand (M) indicate differences between C57BL/6 and *Casp11*$^{-/-}$, or *Casp11*$^{-/-}$, and *Nlrp3*$^{-/-}$ mice, respectively.

This molecule is predominantly expressed in promastigotes, and its synthesis is highly downregulated after differentiation in amastigotes (Turco and Descoteaux, 1992).

The NLRP3 inflammasome was shown to be triggered by multiple species of *Leishmania* (Charmoy et al., 2016; Dey et al., 2018; Gurung et al., 2015; Lefèvre et al., 2013; Lima-Junior et al., 2013), but little is known regarding the signaling pathways that lead to NLRP3 activation in response to *Leishmania*. Here, we found that CASP11 plays an important role in NLRP3 activation and accounts for the inflammasome-mediated restriction of parasite infection. We identified *Leishmania* LPG as an activator of CASP11. Unlike LPS, the LPG-mediated activation of CASP11 is indirect, suggesting the requirement of additional molecules/receptors to allow LPG-mediated activation of CASP11.

RESULTS

CASP11 Contributes to the Control of *Leishmania* spp. Replication in Macrophages and *In Vivo*

CASP11 has been implicated in the non-canonical activation of NLRP3; therefore, we investigated whether CASP11 plays a role in the NLRP3-mediated restriction of *Leishmania* infection. Bone marrow-derived macrophages (BMDMs) from C57BL/6 (wild-type [WT]), *Nlrp3*$^{-/-}$, or *Casp11*$^{-/-}$ mice were infected with metacyclic promastigotes of *Leishmania* at an MOI of 1. Internalization and intracellular parasite loads were determined by Giemsa staining or fluorescence-activated cell sorting (FACS). Although NLRP3 and CASP11 deficiency did not affect internalization of the parasites after 1 hr of infection, it affected intracellular parasite load after 48 or 96 hr. This was observed using many species of *Leishmania*: *L. major* (*L.m.*; Figures 1A and 1B), *L. braziliensis* (*L.b.*; Figures 1C and 1D), and *L. amazonensis* (*L.a.*; Figures 1E and 1F). To further assess the importance of CASP11 for the restriction of *Leishmania* replication in macrophages, we used a strain of *L. amazonensis* expressing GFP and performed flow cytometry using different MOIs (1, 5, and 10). We observed that the parasite loads were higher in *Nlrp3*$^{-/-}$ and *Casp11*$^{-/-}$ cells compared with WT cells, as shown by the percentage of GFP^{+} cells (Figures 1G, 1I, and 1K) and the integrated mean fluorescence intensity (iMFI; Figures 1H, 1J, and 1L). The flow cytometry gating strategy, uninfected cells, and non-GFP-expressing *Leishmania* are shown (Figure S1A). We have previously shown

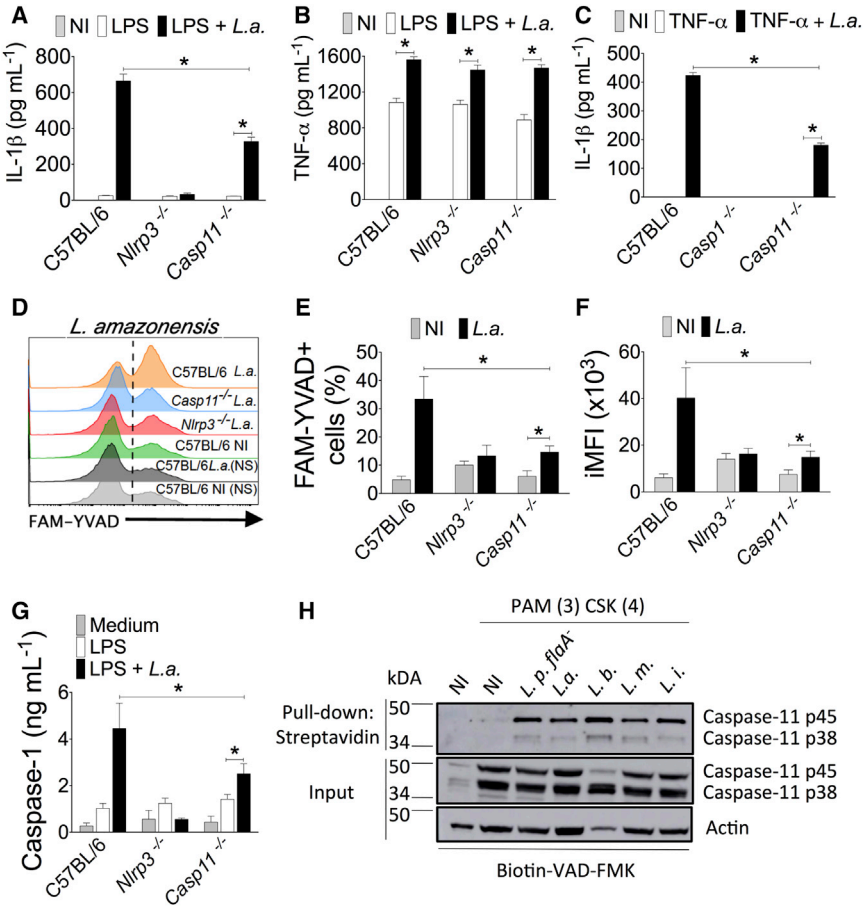

Figure 2. *Leishmania* spp. Trigger Non-canonical Inflammasome Activation in Macrophages

(A–C) Primed BMDMs were infected with stationary-phase *L. amazonensis* promastigotes at an MOI of 10. The levels of IL-1β (A and C) and TNF-α (B) were measured using ELISA.

(D–G) C57BL/6, *Nlrp3*$^{-/-}$, and *Casp11*$^{-/-}$ BMDMs were stained with FAM-YVAD after *L. amazonensis* infection at an MOI of 10, and the percentages of active CASP1-positive cells (E) and the integrated mean fluorescence intensity (iMFI) (F) were evaluated. A representative histogram is shown (D). Cells were infected with *L. amazonensis* (*L.a*) (G), and CASP1 levels were measured in the supernatants using ELISA.

(H) PAM(3)CSK(4)-primed (300 ng mL^{-1}) BMDMs were pre-treated with biotin-VAD-FMK and infected with different *Leishmania* species (MOI 10) or *L. pneumophila flaA*$^{-}$ (positive control). Immunoblotting shows the presence of CASP11 p45 and p38 in the cell lysate (input) and pull-down fractions, representative of activated CASP11. Actin (β-actin) was used as a loading control.

The data are represented as the mean ± SD of triplicate samples (A–I) and are representative of the data obtained from three (A–C) and two (D–H) independent experiments that yielded similar results. Statistical analysis was performed using Student's t test. Asterisks indicate statistically significant differences. *$p < 0.05$.

that NLRP3-mediated restriction of *L. amazonensis* replication in macrophages involves upregulation of NOS2 (Lima-Junior et al., 2013). Thus, we tested if CASP11 affected NOS2 expression in response to infection and found a defective upregulation of NOS2 in *Casp11*$^{-/-}$ and *Nlrp3*$^{-/-}$ BMDMs infected with *L. amazonensis* (Figure S1B). In support of our data indicating that ROS is upstream of inflammasome activation (Lima-Junior et al., 2017), we found that ROS production was independent of CASP11 and NLRP3 (Figure S1C). To test if the CASP11 phenotypes were caused by defective NLRP3 expression, we measured NLRP3 expression in *Casp11*$^{-/-}$ macrophages and found normal NLRP3 expression (Figure S1D).

Next, we used *Nlrp3*$^{-/-}$ and *Casp11*$^{-/-}$ mice to assess the physiological relevance of this pathway for host resistance *in vivo*. WT, *Nlrp3*$^{-/-}$, and *Casp11*$^{-/-}$ mice were intradermally infected in the ear with 10^3 metacyclic promastigotes of *L. amazonensis*, and the infection was monitored for 15 weeks. We found that *Casp11*$^{-/-}$ mice were more susceptible to the disease, as observed by increased ear thickness after the 5th week of infection, similar to that observed in *Nlrp3*$^{-/-}$ mice (Figure 1M). After the 12th week of infection, the lesions in the ears of *Casp11*$^{-/-}$ mice stabilized and were statistically different from those formed in the C57BL/6 and *Nlrp3*$^{-/-}$ mice. Images of the infected ears in the 15th week of infection illustrate the lesion development (Figure 1N), and we found that CASP11 and NLRP3 deficiency resulted in increased parasite loads in the infected ears (Figure 1O). Similar results were obtained when mice were infected with 10^6 stationary-phase promastigotes of *L. amazonensis* (Figures S1E and S1F). Next, we measured activation of the inflammasome *in vivo* in the ears of mice infected with *L. amazonensis*. We detected CASP1 in the ears of the infected mice in the ears of the infected mice, and this process was partially dependent on NLRP3 and CASP11 (Figure S1G).

CASP11 Is Activated during *Leishmania* spp. Infection and Accounts for CASP1 Activation and IL-1β Induction

To evaluate if CASP11 contributes to the non-canonical activation of NLRP3, we infected WT, *Nlrp3*$^{-/-}$, and *Casp11*$^{-/-}$ BMDMs with *L. amazonensis* and quantified IL-1β production. While NLRP3 deficiency abrogated IL-1β production, *Casp11*$^{-/-}$ cells had significantly decreased IL-1β secretion (Figures 2A, S2A, and S2B), but not TNF-α (Figure 2B). Intracellular LPS triggers CASP11 activation; thus, we used TNF-α (Figure 2C) or PAM(3)CSK(4) for priming (Figure S2A) and obtained similar results. Our data indicate that in endotoxin-free conditions, CASP11 is also required for efficient activation of the NLRP3 inflammasome in response to *Leishmania* infection. Furthermore, we found that CASP11 also accounts for the production of IL-1α in response to infection (Figure S2C). The importance of CASP11 for IL-1β production was similarly observed in infections with *L. major* (Figure S2D) and *L. braziliensis* (Figure S2E).

Furthermore, we investigated whether CASP11 was involved in CASP1 activation. We infected BMDMs and evaluated CASP1 activation using FLICA (FAM-YVAD), a cell-permeable dye that binds to the active form of CASP1. We found that NLRP3 and CASP11 are required for efficient CASP1 activation in response to *L. amazonensis* infection (Figures 2D–2F). Similar data were obtained when BMDMs were infected with *L. major* (Figures S2F–S2H) and *L. braziliensis* (Figures S2I–S2K). To further evaluate the effect of CASP11 on CASP1 activation, we quantified CASP1 activation and secretion in response to infection using ELISA. We found that CASP11 is required for efficient CASP1 activation in response to *L. amazonensis* (Figure 2G). Using these three different assays, we unequivocally demonstrate that CASP11 accounts for CASP1 activation and IL-1β secretion; however, we consistently found a CASP11-independent pathway for inflammasome activation in response to infection. We also evaluated the importance of CASP11 for CASP1 activation using western blot. We found that CASP11 is important for CASP1 activation as observed by the production of CASP1 p20 in response to infection with *L. braziliensis*, *L. major*, and *L. amazonensis* (Figures S2L and S2M).

Next, we evaluated CASP11 activation directly by pulling down active CASP11 from infected cells, as previously described (Cunha et al., 2015). We found that CASP11 is activated in response to several species of *Leishmania*, as shown in the pull-down blot (Figure 2H). The flagellin mutant *Legionella pneumophila (L.p. flaA^{-})* triggers potent activation of CASP11 and was used as a positive control in this experiment.

Leishmania LPG Triggers CASP11 Activation in BMDMs, Resulting in Cell Death and IL-β Release

Parasites from the *Leishmania* genus display several glycoconjugates and proteins that have been described as virulence factors. Among those, the most abundant glycoconjugate on the *Leishmania* surface is LPG, which provides a sugar coat that protects the microbes in different environments, similar to bacterial LPS (de Assis et al., 2012; Turco and Descoteaux, 1992). CASP11 is activated by LPS; thus, we hypothesized that LPG could be involved in CASP11 activation in response to *Leishmania* species. Initially, we compared the production of IL-1β in BMDMs infected with *L. amazonensis* promastigotes or amastigotes, which highly downregulate LPG expression (de Assis et al., 2012; Turco and Descoteaux, 1992). We found that whereas promastigotes induce robust CASP11-dependent inflammasome activation, the amastigotes induce less potent inflammasome activation (Figure S3A). Furthermore, we tested the effect of LPG on inflammasome activation. C57BL/6 macrophages were transfected with endotoxin-free highly purified *Leishmania* LPG. Upon DOTAP transfection, LPG from *L. amazonensis* (Figure 3A), *L. major* (Figure 3B), and *L. donovani* (*L.d.*; Figure 3C) induced IL-1β production in a dose-dependent manner. *E. coli* LPS was used as a positive control (Hagar et al., 2013; Kayagaki et al., 2013). As expected, no IL-1β was detected when cells were treated with LPS or LPG in the absence of DOTAP. We found that LPG transfection also induced CASP1 cleavage as measured using western blot (Figure 3D). As a control for LPS contamination in our LPG samples, we quantified endotoxin levels in purified LPGs using a *Limulus* amebocyte lysate (LAL) assay kit, and the concentration of LPS in all samples tested was below the detection limit (data not shown). In addition, we evaluated the LPG samples using mass spectrometry and found that the LPG was free of contamination with polar and non-polar peptides (data not shown). Next, we transfected LPG in C57BL/6, *Nlrp3*$^{-/-}$, *Casp11*$^{-/-}$, and *Casp1/11*$^{-/-}$ BMDMs and quantified IL-1β production. We found that *L. major*, *L. amazonensis*, and *L. donovani* LPG induced robust IL-1β production in C57BL/6 but not in *Nlrp3*$^{-/-}$, *Casp11*$^{-/-}$, or *Casp1/11*$^{-/-}$ cells (Figure 3E), confirming that intracellular LPG triggers CASP11-dependent activation of NLRP3. CASP11 activation by LPS induces pore formation in BMDMs (Case et al., 2013; Hagar et al., 2013; Kayagaki et al., 2013). Thus, we tested if LPG transfection is sufficient to induce pore formation by assessing the influx of propidium iodide. We found that LPG from *L. amazonensis*, *L. major*, and *L. donovani* induced robust pore formation after 1 hr of transfection of C57BL/6 macrophages (Figure 3F). NLRP3 was dispensable for pore formation induced by LPG, but the pore formation was abrogated in *Casp11*$^{-/-}$ and *Casp1/11*$^{-/-}$ BMDMs (Figure 3F). When cell death was measured by assessing LDH release, intracellular (DOTAP-transfected) but not extracellular LPG triggered cell death as measured by LDH release (Figure 3G). In addition, LPG from *L. amazonensis*, *L. major*, and *L. donovani* induced CASP11-dependent cell death upon transfection (Figure 3H). To further assess the activation of CASP11 by LPG in C57BL/6 macrophages, active CASP11 was pulled down following LPG transfection. Neither PAM(3)CSK(4) priming alone nor stimulation with extracellular LPG induced CASP11 activation; however, transfection of LPG from several *Leishmania* species resulted in robust CASP11 activation, closely resembling the activation induced by LPS (Figure 3I).

It was previously shown that LPS binds directly and activates mouse CASP11 and human Casp4/5 *in vitro* (Shi et al., 2014). Thus, we investigated whether LPG functions similarly to LPS to induce Casp4 and CASP11 activation. First, we evaluated if LPGs could activate Casp4 expressed and purified from insect cells. Although LPS (used as a positive control) induces strong Casp4 activity, LPG from neither *L. amazonensis* nor *L. braziliensis* could induce Casp4 activation (Figure S3B). Next, we performed a competition assay using unlabeled LPS or *Leishmania* LPGs to compete with biotinylated LPS, as previously described (Shi et al., 2014). Cell lysates from HEK293T cells stably expressing Flag-tagged CASP11 (C/A) were first incubated with unlabeled LPS or LPGs and further incubated with biotinylated LPS, followed by pull-down with streptavidin beads. We found that unlabeled LPS, but not LPGs, competed with biotinylated LPS for CASP11 binding (Figure S3C). Taken together, these assays show that in a cell-free system, *Leishmania* LPG fails to directly bind or activate human Casp4 or mouse CASP11, suggesting that the CASP11 activation in response to *Leishmania* LPG may be indirect and require additional molecules present in the macrophage cytoplasm.

A Leishmania major Mutant Lacking LPG (*Lpg1*$^{-/-}$) Is Unable to Trigger the CASP11-Mediated Non-canonical Activation of the NLRP3 Inflammasome

To evaluate the role of LPG in inflammasome activation during *Leishmania* infection, we used an *L. major* strain deficient for

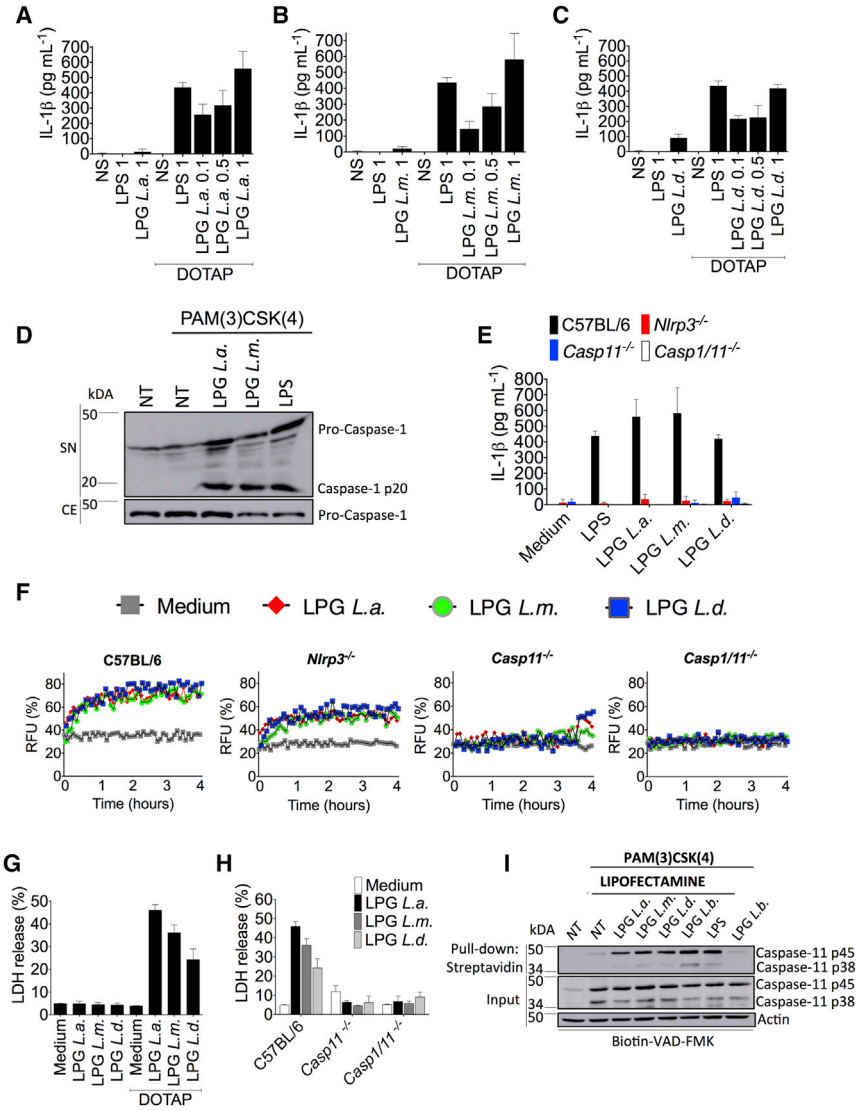

Figure 3. Lipophosphoglycan from *Leishmania* spp. Induces Non-canonical Inflammasome Activation in Macrophages

(A–C) BMDMs were primed with PAM(3)CSK(4) (300 ng mL^{-1}), transfected with lipophosphoglycan (LPG) from *L. amazonensis* (A), *L. major* (*L.m.*) (B), *or L. donovani* (*L.d.*) (C) at increasing concentrations (0.1, 0.5, or 1.0 μg mL^{-1}), or treated with LPS. LPG and LPS (1.0 μg mL^{-1}) were also added extracellularly. IL-1β was measured in cell-free supernatants using ELISA.

(D) Western blotting indicating the presence of casp-1 in supernatants (SN) and in the cellular extract (CE) of BMDMs transfected with different LPGs or LPS (1 μg mL^{-1}).

(E–H) C57BL/6, *Nlrp3*$^{-/-}$, *Casp11*$^{-/-}$, and *Casp1/11*$^{-/-}$ BMDMs were primed with PAM(3)CSK(4) and transfected with LPG from different *Leishmania* species. IL-1β levels were quantified using ELISA (E), pore formation was assessed fluorometrically in real time by the uptake of propidium iodide (RFUs [relative fluorescence units]) (F), and cell death was evaluated by LDH release (G and H).

(I) Immunoblotting shows the presence of CASP11 p45 and p38 in the cell lysate (input) and its active form in the pull-down fraction of C57BL/6 BMDMs transfected with different LPGs. LPG *L. braziliensis* (*L.b.*) was used as an extracellular negative control and transfected LPS as a positive control. β-Actin was used as a loading control.

The data are represented as the mean ± SD of triplicate samples and are representative of the data obtained from at least three (A–C, E, G, and H) and two (D, F, and I) independent experiments.

LPG (*Lpg1*$^{-/-}$). This arose through deletion of all copies of the *Lpg1* gene, which encodes a galactofuranosyl (Galf) transferase required for biosynthesis of the LPG glycan core (Späth et al., 2000, 2003). Thus, *L. major Lpg1*$^{-/-}$ parasites lack LPG but synthesize normal levels of other related glycoconjugates and GPI-anchored proteins and are a reliable model to evaluate the role of LPG in the immune response against the parasite (reviewed by Franco et al., 2012). To evaluate the effect of LPG on CASP1 activation, BMDMs from C57BL/6, *Nlrp3*$^{-/-}$, and *Casp11*$^{-/-}$ mice were infected with *L. major* WT and isogenic controls. The strains used included Lpg1 null (*Lpg1*$^{-/-}$) and *Lpg1*$^{-/-}$ complemented with the *Lpg1* gene, which generates the add-back strain (*Lpg1*$^{-/-}$/+*Lpg1*). By performing the FLICA assay, we found that *Lpg1*$^{-/-}$ had an impaired ability to trigger CASP1 activation compared with WT or the complemented strain (Figures 4A–4C). This effect was fully dependent on NLRP3 and largely dependent on CASP11. We measured CASP1 p20 using western blot and found that CASP1 cleavage was decreased in response to *Lpg1*$^{-/-}$ parasites, but this effect was null in *Casp11*$^{-/-}$ BMDMs (Figure 4D). Furthermore, we measured IL-1β using ELISA and found that IL-1β production was reduced in response to *L. major Lpg1*$^{-/-}$ parasites in C57BL/6 but not *Casp11*$^{-/-}$ macrophages (Figures 4E and 4F). This was evident when cells were primed with LPS (Figure 4E) or PAM(3)CSK(4) (Figure 4F). These effects were not due to defective internalization of the parasites, as the percentage of infected cells (Figure S4A) and the average numbers of parasites per cell (Figure S4B) were similar between the clones at 1 hr post-infection.

Next, we performed a pull-down assay in C57BL/6 macrophages to evaluate CASP11 activation in response to infection with *L. major Lpg1*$^{-/-}$ and *Lpg1*$^{-/-}$/+*Lpg1*. We found that *L. major Lpg1*$^{-/-}$ did not trigger robust CASP11 activation in response to infection (Figure 4G). Finally, we assessed the effects of LPG and CASP11 in the expression of *Nos2*, a process that was previously shown to be dependent on NLRP3 (Lima-Junior et al., 2013). We infected C57BL/6, *Nlrp3*$^{-/-}$, and *Casp11*$^{-/-}$ with *L. major Lpg1*$^{-/-}$ and *Lpg1*$^{-/-}$/+*Lpg1* and found that the upregulation of *Nos2* but not *Tnfa* requires LPG, NLRP3, and CASP11 (Figures 4H and 4I). Taken together these results demonstrate that *Leishmania* LPG accounts for

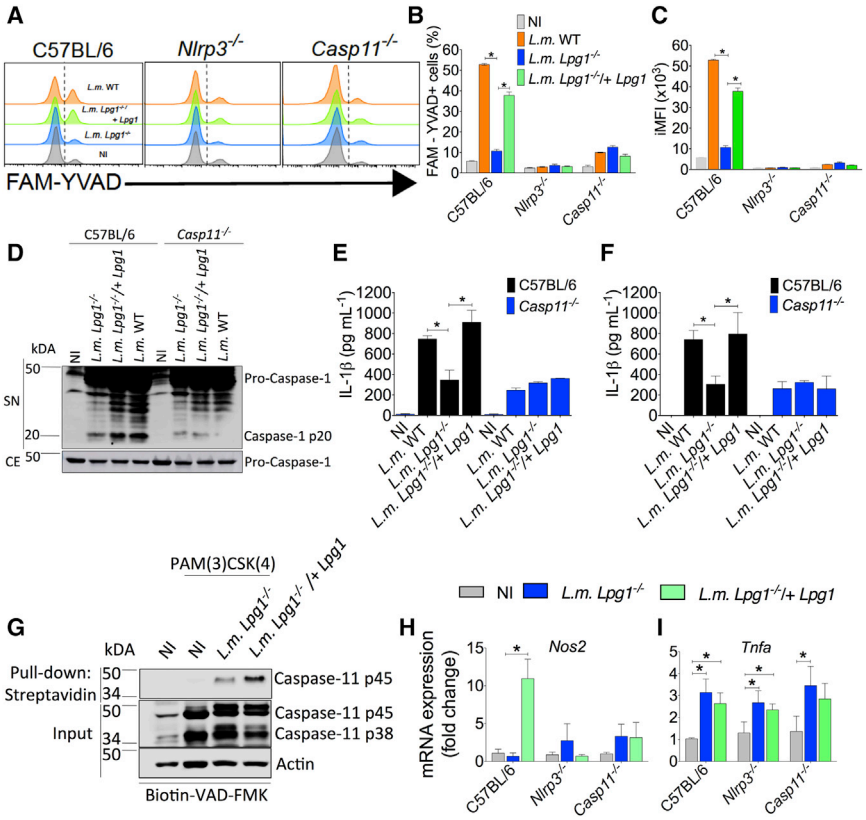

Figure 4. LPG Deficiency Impairs Non-canonical Inflammasome Activation by *Leishmania major*

(A–C) WT, *Nlrp3*$^{-/-}$, and *Casp11*$^{-/-}$ BMDMs were infected with stationary-phase *L. major* WT, *L. major Lpg1*$^{-/-}$, or *L. major Lpg1*$^{-/-}$/+*Lpg1* at an MOI of 10. Cells were stained for FAM-YVAD and analyzed using flow cytometry to determine the percentage of FAM-YVAD-positive cells (B) and the integrated mean fluorescence intensity (iMFI) (C). A representative histogram is shown (A).

(D) Western blotting analysis of WT and *Casp11*$^{-/-}$ BMDMs infected with *L. m.* mutants at an MOI of 10, indicating the presence of casp-1 p45 and casp-1 p20 in the cell-free culture supernatants (SN) and casp-1 p45 in the cellular extract (CE).

(E and F) WT and *Casp11*$^{-/-}$ BMDMs were primed with LPS (E) or PAM(3)CSK(4) (F) and infected with stationary-phase *L. major* WT and mutants at an MOI of 10. IL-1β levels in cell-free supernatants were measured using ELISA.

(G) WT BMDMs were primed with PAM(3)CSK(4) pre-treated with biotin-VAD-FMK and infected with stationary-phase *L. major* mutants at an MOI of 10. The pull-down for active CASP11 was performed as previously described.

(H and I) WT, *Nlrp3*$^{-/-}$, and *Casp11*$^{-/-}$ BMDMs were infected with stationary-phase *L. major Lpg1*$^{-/-}$ or *L. major Lpg1*$^{-/-}$/+*Lpg1* at an MOI of 10. After 3 hr of infection, RNA was extracted, and qPCR for the *Nos2* (H) and *Tnfa* (I) genes were performed.

The data are shown as the mean ± SD of triplicate samples (A–C, E, and F) and are representative of data obtained from at least three or two (D and G) independent experiments. Statistical analysis was performed using Student's t test. Asterisks indicate statistically significant differences. *p < 0.05.

CASP11 activation and promotes the non-canonical activation of the NLRP3 inflammasome.

DISCUSSION

Activation of the NLRP3 inflammasome has been reported to affect the outcome of leishmaniasis in humans and in mouse models of infection (Charmoy et al., 2016; Gurung et al., 2015; Lima-Junior et al., 2013, 2017; Novais et al., 2018). We and others have shown that the inflammasome is protective and accounts for the restriction of parasite replication in macrophages and *in vivo* (Lefèvre et al., 2013; Lima-Junior et al., 2013, 2017; Miranda et al., 2015; Sani et al., 2014; Santos et al., 2013). Consistent with this hypothesis, others have shown that certain *Leishmania* species actively inhibit activation of the inflammasome (Gupta et al., 2017; Hartley et al., 2018; Shio et al., 2015). However, these findings do not conflict with studies demonstrating that the inflammasome (via IL-1β) promotes inflammation and pathology (Charmoy et al., 2016; Dey et al., 2018; Gurung et al., 2015; Novais et al., 2018; Santos et al., 2018). It is likely that these two processes occur concomitantly; while inflammasome-induced inflammation contributes to pathology, it also accounts for induction of protective immunity that limits parasite replication. Interestingly, it was reported that the NLRP3 inflammasome contributes to the generation of CD8$^+$ T cell-mediated cytotoxicity (Charmoy et al., 2016; Dey et al., 2018; Gurung et al., 2015; Novais et al., 2018; Santos et al., 2018), an observation that agrees with the vast literature indicating that adaptive immunity is critical for the outcome of the disease (reviewed in Broz and Dixit, 2016; Zamboni and Lima-Junior, 2015). In this context, it is possible that CASP11 also influences the generation of adaptive responses during leishmaniasis. This hypothesis is particularly supported by the fact that *in vivo* phenotypes of the *Casp11*$^{-/-}$ mice are only evident after the fourth to fifth week of infection, when adaptive immunity is well established. Nonetheless, our macrophage experiments unequivocally support a role of CASP11 and NLRP3 in innate responses that operates in the absence of lymphocytes and adaptive immunity.

Despite the clear importance of the inflammasome for the outcome of disease, little is known about the mechanism by which NLRP3 is activated during *Leishmania* infection. ROS production via dectin-1 and K$^+$ efflux were shown to be involved (Lefèvre et al., 2013; Lima-Junior et al., 2013, 2017), but further mechanisms are unknown. Herein, we identified that CASP11 is strongly activated by *Leishmania* LPG and leads to the non-canonical activation of NLRP3. As opposed to LPS, which binds CASP11 directly to induce its activation (Shi et al., 2014), *Leishmania* LPG fails to physically interact with CASP11 (or with human Casp4) in a cell-free system. Nonetheless, transfection of highly purified

LPG in macrophages (in concentrations equivalent to those used for LPS) is sufficient to trigger CASP11 activation, suggesting that additional macrophage molecules or receptors may participate in this process. Importantly, LPG-mediated CASP11 activation is not due to LPS contamination. Our LPG was purified directly from *Leishmania* in endotoxin-free conditions, and we detected neither endotoxin nor protein contamination in our LPG preparations. In addition, a possible LPS contamination in our LPG preparations would lead to CASP11 activation in the cell-free system experiment, which was not observed (Figure S3). Furthermore, our experiments with *Lpg1*$^{-/-}$, which were all performed in endotoxin-free conditions, support our assertion that regardless of LPS contamination, LPG triggers CASP11 activation. It is worth mentioning that our experiments using LPG mutant parasites were performed using an available strain of *L. major* (Späth et al., 2000, 2003). Although the effects of the inflammasome in the outcome of the disease *in vivo* may be different in *L. major* and *L. amazonensis*, the induction of inflammasome activation in macrophages is similar in all species tested, including *L major* (Charmoy et al., 2016; Gurung et al., 2015; Lima-Junior et al., 2013, 2017; Novais et al., 2018). These findings support the use of *L. major Lpg1*$^{-/-}$ to assess the effect of CASP11 in the activation of the NLRP3 inflammasome in macrophages. Of note, experiments *in vivo* using LPG-deficient parasites cannot be achieved, because LPG is essential for parasite replication in macrophages and *in vivo*. Interestingly, LPG expression is highly down modulated when the intracellular parasites become amastigotes (Turco and Descoteaux, 1992). These findings are in agreement with our data showing that axenic amastigotes induce less CASP11 activation then promastigotes (Figure S3A). One can speculate that this has been evolutionary selected to limit inflammasome activation during mammalian infection. Nonetheless, the amastigotes still express a small amount of LPG (McConville and Blackwell, 1991), a feature that supports our findings that amastigotes still trigger CASP11-dependent inflammasome activation in macrophages (Figure S3A). This may explain our *in vivo* data, where we detected an important role for CASP11 after up to 15 weeks of infection (Figures 1M–1O).

Although LPG was reported to trigger TLR activation, most of the literature supports an anti-inflammatory role for this molecule (de Assis et al., 2012; Franco et al., 2012; Matte and Descoteaux, 2016). Our data indicate that extracellular LPG does not promote inflammasome activation. However, when LPG is delivered in the cytosol, it strongly triggers CASP11 activation. It is unclear if this host response specifically evolved to detect intracellular *Leishmania* or whether this is actively modulated by *Leishmania* to favor disease chronification and transmission. It is also unclear how LPG accesses the macrophage cytosol to engage CASP11 activation. It is possible that LPG sheds and reaches the host cell cytoplasm through the release of exosomes before or after macrophage infection (Silverman et al., 2010). Another possibility is that LPG is actively translocated to the host cell cytoplasm to promote an inflammatory environment that, under certain conditions, may favor parasite persistence and transmission (Charmoy et al., 2016; Gurung et al., 2015; Novais et al., 2018; Santos et al., 2018). Finally, it is also possible that this glycoconjugate is accidentally translocated to the host cell cytoplasm during parasite manipulation of macrophage functions, a process that is still highly underappreciated despite the clinical importance of this disease. Regardless of these speculations, our findings link LPG to NLRP3 activation via the CASP11-mediated non-canonical pathway. These findings help unravel the roles of CASP11 in immunity and account for our understanding of the pathogenesis and host response to this important pathogen that infects millions of people worldwide.

STAR★METHODS

Detailed methods are provided in the online version of this paper and include the following:

- KEY RESOURCES TABLE
- CONTACT FOR REAGENT AND RESOURCE SHARING
- EXPERIMENTAL MODEL AND SUBJECT DETAILS
  - Animals
  - Parasite culture and infection *in vivo*
- METHOD DETAILS
  - Extraction and purification of LPG
  - Bone marrow-derived macrophages and infection
  - Transfection experiments
  - Cell death assay
  - Membrane pore formation assay
  - Endotoxin detection
  - ROS detection
  - *In vivo* detection of CASP1
  - ELISA assay
  - Endogenous CASP1 staining
  - Western blot
  - Casp4 activity assay
  - Active CASP11 and LPG binding pull-down assay
  - Real-time PCR
- QUANTIFICATION AND STATISTICAL ANALYSIS
  - Statistical analysis

SUPPLEMENTAL INFORMATION

Supplemental Information includes four figures and can be found with this article online at https://doi.org/10.1016/j.celrep.2018.12.047.

ACKNOWLEDGMENTS

We would like to thank Maira Nakamura for technical support. We are grateful to Richard Flavell (Yale) for providing the *Casp1/11*$^{-/-}$ mice and to Vishva Dixit (Genentech) for providing the *Nlrp3*$^{-/-}$, *Casp11*$^{-/-}$, and *Casp1/11*$^{-/-}$/*Casp11*^{Tg} mice and the anti-CASP1 p20 antibody. This work was supported by grants from PEW, Training in Tropical Diseases/World Health Organization (TDR/WHO), FAEPA, INCTV/CNPq, CNPq (grants 401577/2014-7 and 445881/2014-3), and CRID/FAPESP and FAPESP (grants 2013/08216-2 and 2014/04684-4). R.P.S. was supported by FAPEMIG (grants PPM-X 00102-16 and PPM-X 00102-16) and S.M.B. was supported by NIH grant R01 AI031078. R.V.H.C., W.A.A., and D.S.L.-J. were supported by fellowships from FAPESP. D.S.Z. and R.P.S. are Research Fellows from CNPq.

AUTHOR CONTRIBUTIONS

R.V.H.C. and W.A.A. designed and performed the experiments, analyzed the data, generated the figures, and wrote the manuscript. D.S.L.-J., M.D., C.V.O., K.W., and F.S. designed and performed the experiments and helped

with data interpretation. P.M.N., J.N.R., R.P.S., and S.M.B. provided reagents, helped with data interpretation, and discussed the hypotheses. S.M.B. and R.P.S. assisted in manuscript revisions. D.S.Z. supervised the project, designed the experiments, helped with data interpretation, participated in the data analysis, and wrote the manuscript.

DECLARATION OF INTERESTS

The authors declare no competing interests.

Received: April 11, 2018
Revised: September 7, 2018
Accepted: December 11, 2018
Published: January 8, 2019

REFERENCES

Alvar, J., Vélez, I.D., Bern, C., Herrero, M., Desjeux, P., Cano, J., Jannin, J., and den Boer, M.; WHO Leishmaniasis Control Team (2012). Leishmaniasis worldwide and global estimates of its incidence. PLoS ONE *7*, e35671.

Broz, P., and Dixit, V.M. (2016). Inflammasomes: mechanism of assembly, regulation and signalling. Nat. Rev. Immunol. *16*, 407–420.

Case, C.L., Kohler, L.J., Lima, J.B., Strowig, T., de Zoete, M.R., Flavell, R.A., Zamboni, D.S., and Roy, C.R. (2013). Caspase-11 stimulates rapid flagellin-independent pyroptosis in response to Legionella pneumophila. Proc. Natl. Acad. Sci. U S A *110*, 1851–1856.

Chappuis, F., Sundar, S., Hailu, A., Ghalib, H., Rijal, S., Peeling, R.W., Alvar, J., and Boelaert, M. (2007). Visceral leishmaniasis: what are the needs for diagnosis, treatment and control? Nat. Rev. Microbiol. *5*, 873–882.

Charmoy, M., Hurrell, B.P., Romano, A., Lee, S.H., Ribeiro-Gomes, F., Riteau, N., Mayer-Barber, K., Tacchini-Cottier, F., and Sacks, D.L. (2016). The Nlrp3 inflammasome, IL-1β, and neutrophil recruitment are required for susceptibility to a nonhealing strain of Leishmania major in C57BL/6 mice. Eur. J. Immunol. *46*, 897–911.

Cunha, L.D., Ribeiro, J.M., Fernandes, T.D., Massis, L.M., Khoo, C.A., Moffatt, J.H., Newton, H.J., Roy, C.R., and Zamboni, D.S. (2015). Inhibition of inflammasome activation by Coxiella burnetii type IV secretion system effector IcaA. Nat. Commun. *6*, 10205.

de Assis, R.R., Ibraim, I.C., Nogueira, P.M., Soares, R.P., and Turco, S.J. (2012). Glycoconjugates in New World species of Leishmania: polymorphisms in lipophosphoglycan and glycoinositolphospholipids and interaction with hosts. Biochim. Biophys. Acta *1820*, 1354–1365.

Dey, R., Joshi, A.B., Oliveira, F., Pereira, L., Guimaraes-Costa, A.B., Serafim, T.D., de Castro, W., Coutinho-Abreu, I.V., Bhattacharya, P., Townsend, S., et al. (2018). Gut microbes egested during bites of infected sand flies augment severity of leishmaniasis via inflammasome-derived IL-1beta. Cell Host Microbe *23*, 134–143.e6.

Franco, L.H., Beverley, S.M., and Zamboni, D.S. (2012). Innate immune activation and subversion of Mammalian functions by leishmania lipophosphoglycan. J. Parasitol. Res. *2012*, 165126.

Gupta, A.K., Ghosh, K., Palit, S., Barua, J., Das, P.K., and Ukil, A. (2017). *Leishmania donovani* inhibits inflammasome-dependent macrophage activation by exploiting the negative regulatory proteins A20 and UCP2. FASEB J. *31*, 5087–5101.

Gurung, P., Karki, R., Vogel, P., Watanabe, M., Bix, M., Lamkanfi, M., and Kanneganti, T.D. (2015). An NLRP3 inflammasome-triggered Th2-biased adaptive immune response promotes leishmaniasis. J. Clin. Invest. *125*, 1329–1338.

Hagar, J.A., Powell, D.A., Aachoui, Y., Ernst, R.K., and Miao, E.A. (2013). Cytoplasmic LPS activates caspase-11: implications in TLR4-independent endotoxic shock. Science *341*, 1250–1253.

Hartley, M.A., Eren, R.O., Rossi, M., Prevel, F., Castiglioni, P., Isorce, N., Desponds, C., Lye, L.F., Beverley, S.M., Drexler, S.K., and Fasel, N. (2018). *Leishmania guyanensis* parasites block the activation of the inflammasome by inhibiting maturation of IL-1β. Microb. Cell *5*, 137–149.

Kayagaki, N., Warming, S., Lamkanfi, M., Vande Walle, L., Louie, S., Dong, J., Newton, K., Qu, Y., Liu, J., Heldens, S., et al. (2011). Non-canonical inflammasome activation targets caspase-11. Nature *479*, 117–121.

Kayagaki, N., Wong, M.T., Stowe, I.B., Ramani, S.R., Gonzalez, L.C., Akashi-Takamura, S., Miyake, K., Zhang, J., Lee, W.P., Muszyński, A., et al. (2013). Noncanonical inflammasome activation by intracellular LPS independent of TLR4. Science *341*, 1246–1249.

Kaye, P., and Scott, P. (2011). Leishmaniasis: complexity at the host-pathogen interface. Nat. Rev. Microbiol. *9*, 604–615.

Lefèvre, L., Lugo-Villarino, G., Meunier, E., Valentin, A., Olagnier, D., Authier, H., Duval, C., Dardenne, C., Bernad, J., Lemesre, J.L., et al. (2013). The C-type lectin receptors dectin-1, MR, and SIGNR3 contribute both positively and negatively to the macrophage response to Leishmania infantum. Immunity *38*, 1038–1049.

Lima-Junior, D.S., Costa, D.L., Carregaro, V., Cunha, L.D., Silva, A.L., Mineo, T.W., Gutierrez, F.R., Bellio, M., Bortoluci, K.R., Flavell, R.A., et al. (2013). Inflammasome-derived IL-1β production induces nitric oxide-mediated resistance to Leishmania. Nat. Med. *19*, 909–915.

Lima-Junior, D.S., Mineo, T.W.P., Calich, V.L.G., and Zamboni, D.S. (2017). Dectin-1 activation during *Leishmania amazonensis* phagocytosis prompts Syk-dependent reactive oxygen species production to trigger inflammasome assembly and restriction of parasite replication. J. Immunol. *199*, 2055–2068.

Mariathasan, S., Weiss, D.S., Newton, K., McBride, J., O'Rourke, K., Roose-Girma, M., Lee, W.P., Weinrauch, Y., Monack, D.M., and Dixit, V.M. (2006). Cryopyrin activates the inflammasome in response to toxins and ATP. Nature *440*, 228–232.

Matte, C., and Descoteaux, A. (2016). Exploitation of the host cell membrane fusion machinery by Leishmania is part of the infection process. PLoS Pathog. *12*, e1005962.

McConville, M.J., and Blackwell, J.M. (1991). Developmental changes in the glycosylated phosphatidylinositols of Leishmania donovani. Characterization of the promastigote and amastigote glycolipids. J. Biol. Chem. *266*, 15170–15179.

Miranda, M.M., Panis, C., da Silva, S.S., Macri, J.A., Kawakami, N.Y., Hayashida, T.H., Madeira, T.B., Acquaro, V.R., Jr., Nixdorf, S.L., Pizzatti, L., et al. (2015). Kaurenoic acid possesses leishmanicidal activity by triggering a NLRP12/IL-1β/cNOS/NO pathway. Mediators Inflamm. *2015*, 392918.

Novais, F.O., Wong, A.C., Villareal, D.O., Beiting, D.P., and Scott, P. (2018). $CD8^+$ T cells lack local signals to produce IFN-γ in the skin during *Leishmania* infection. J. Immunol. *200*, 1737–1745.

Reithinger, R., Dujardin, J.C., Louzir, H., Pirmez, C., Alexander, B., and Brooker, S. (2007). Cutaneous leishmaniasis. Lancet Infect. Dis. *7*, 581–596.

Sani, M.R., Moghaddam, M.M., Aghamollaei, H., Hassanpour, K., Taheri, R.A., and Farnoosh, G. (2014). Investigation of caspase-1 activity and interleukin-1beta production in murine macrophage cell lines infected with Leishmania major. Asian Pac. J. Trop. Med. *7S1*, S70–S73.

Santos, D.M., Carneiro, M.W., de Moura, T.R., Soto, M., Luz, N.F., Prates, D.B., Irache, J.M., Brodskyn, C., Barral, A., Barral-Netto, M., et al. (2013). PLGA nanoparticles loaded with KMP-11 stimulate innate immunity and induce the killing of Leishmania. Nanomedicine (Lond.) *9*, 985–995.

Santos, D., Campos, T.M., Saldanha, M., Oliveira, S.C., Nascimento, M., Zamboni, D.S., Machado, P.R., Arruda, S., Scott, P., Carvalho, E.M., and Carvalho, L.P. (2018). IL-1β production by intermediate monocytes is associated with immunopathology in cutaneous leishmaniasis. J. Invest. Dermatol. *138*, 1107–1115.

Shi, J., Zhao, Y., Wang, Y., Gao, W., Ding, J., Li, P., Hu, L., and Shao, F. (2014). Inflammatory caspases are innate immune receptors for intracellular LPS. Nature *514*, 187–192.

Shio, M.T., Christian, J.G., Jung, J.Y., Chang, K.P., and Olivier, M. (2015). PKC/ROS-mediated NLRP3 inflammasome activation is attenuated by Leishmania zinc-metalloprotease during infection. PLoS Negl. Trop. Dis. *9*, e0003868.

Silverman, J.M., Clos, J., Horakova, E., Wang, A.Y., Wiesgigl, M., Kelly, I., Lynn, M.A., McMaster, W.R., Foster, L.J., Levings, M.K., and Reiner, N.E. (2010). Leishmania exosomes modulate innate and adaptive immune responses through effects on monocytes and dendritic cells. J. Immunol. *185*, 5011–5022.

Späth, G.F., Epstein, L., Leader, B., Singer, S.M., Avila, H.A., Turco, S.J., and Beverley, S.M. (2000). Lipophosphoglycan is a virulence factor distinct from related glycoconjugates in the protozoan parasite Leishmania major. Proc. Natl. Acad. Sci. U S A *97*, 9258–9263.

Späth, G.F., Lye, L.F., Segawa, H., Sacks, D.L., Turco, S.J., and Beverley, S.M. (2003). Persistence without pathology in phosphoglycan-deficient Leishmania major. Science *301*, 1241–1243.

Turco, S.J., and Descoteaux, A. (1992). The lipophosphoglycan of Leishmania parasites. Annu. Rev. Microbiol. *46*, 65–94.

World Health Organization (2010). Control of the Leishmaniases. WHO Technical Report Series (Geneva: World Health Organization), pp. 22–26.

Zamboni, D.S., and Lima-Junior, D.S. (2015). Inflammasomes in host response to protozoan parasites. Immunol. Rev. *265*, 156–171.

STAR★METHODS

KEY RESOURCES TABLE

REAGENT OR RESOURCE	SOURCE	IDENTIFIER
Antibodies		
Mouse Anti-Flag	Sigma-Aldrich	F3165; RRID:AB_259529
Rat Anti-Caspase-1 (clone 4B4)	Genentech	N/A
Rabbit Anti-Caspase-11	Abcam	ab180673
Anti-NLRP3/NALP3 mAb (Cryo-2)	AdipoGen	Cat# AG-20B-0014; RRID:AB_2490202
Mouse Anti-β-Actin (C4)	Santa Cruz	sc-47778; RRID:AB_2714189
Chemicals, Peptides and Recombinant proteins		
Puromycin	Sigma-Aldrich	P8833-10MG
Geneticin (G418)	Sigma-Aldrich	A1720
Hygromycin B	InvivoGen	ant-hg-1
Pam3CSK4	InvivoGen	tlrl-pms
Ultrapure LPS	InvivoGen	tlrl-3pelps
Biotinylated-LPS	InvivoGen	Tlrl-3blps
Propidium Iodide	Sigma-Aldrich	CAS25535-16-4
Mouse TNF-α Recombinat Protein	eBioscience	34-8321-63
Lipofectamine 2000	Invitrogen	11668027
DOTAP	Roche	11 202 375 001
Ac-WEHD-AFC	Enzo Life Sciences	ALX-260-117
Biotin-VAD-FMK	Cayman Chemicals	1135688-15-1
LIVE/DEAD Violet fluorescent reactive dye	Invitrogen	L34964
Protease inhibitor cocktail	Roche	11 836 153 001
streptavidin-agarose beads	Invitrogen	SA10004
streptavidin-Sepharose beads	Sigma-Aldrich	GE17-5113-01
LPG from *L. amazonensis*	This study	N/A
LPG from *L. major*	This study	N/A
LPG from *L. brazilienis*	This study	N/A
Critical commercial assays		
Mouse TNF (Mono/Mono) ELISA Set	BD Bioscience	555268
Mouse IL-1β/IL-1F2 DuoSet	R&D Systems	DY401-05
FAM-FLICA Caspase-1 Assay Kit	Immunochemistry Technologies	98
Limulus Amebocyte Lysate (LAL) assay kit - QCL-1000	Lonza	50-647U
CytoTox 96 Non-Radioactive Cytotoxicity Assay kit	Promega	G1780
Caspase-1 (mouse) Elisa Kit	Adipogen	AG-45B-0002KI01
Experimental Models: Cell Lines		
HEK293	ATCC	ATCC CRL-1573
L-929	ATCC	ATCC CCL-1
Experimental Models: Organism/Strains		
C57BL/6J mice	Jackson Labs	000664
Caspase-11 Knockout mice	Kayagaki et al., 2011	N/A
NLRP3 Knockout mice	Mariathasan et al., 2006	N/A
Casp1$^{-/-}$ (*Casp1/11*$^{-/-}$/*Casp11*^{Tg}) Knockout mice	Kayagaki et al., 2011	N/A
Leishmania (L.) amazonensis M2269 strain (MHOM/BR/73/M2269)	Lima-Junior et al., 2013	N/A
Leishmania (L.) amazonensis PH8 strain (IFLA/BR/67/PH8)	Lima-Junior et al., 2013	N/A

(*Continued on next page*)

Continued

REAGENT OR RESOURCE	SOURCE	IDENTIFIER
Leishmania (V.) braziliensis M2903 strain (MHOM/BR/75/M2903)	Lima-Junior et al., 2013	N/A
Leishmania (L.) major LV39 strain (MRHO/SU/59/P	Lima-Junior et al., 2013	N/A
Leishmania (L.) major LV39c5 *Lpg1*$^{-/-}$ mutant strain (M3P6)	Späth et al., 2000	N/A
Leishmania (L.) major LV39c5 *Lpg1*$^{-/-}$/+*Lpg1* mutant strain (M3P4)	Späth et al., 2000	N/A
Leishmania (L.) infantum (HU-USF 8)	Lima-Junior et al., 2013	N/A
Oligonucleotides		
HPRT forward	Lima-Junior et al., 2013	TCAGTCAACGGGGGACATAAA
HPRT reverse	Lima-Junior et al., 2013	AAGCCATGCCAATGTTGTCT
Nos2 forward	Lima-Junior et al., 2013	CGAAACGCTYCACTTCCAA
Nos2 reverse	Lima-Junior et al., 2013	CGAAACGCTYCACTTCCAA
Tnfa forward	Lima-Junior et al., 2013	TGTGCTCAGAGCTTTCAACAA
Tnfa reverse	Lima-Junior et al., 2013	CTTGATGGTGGTGCATGAGA
Software and Algorithms		
FlowJo Tree Star software	FlowJo LLC	https://www.flowjo.com/solutions/flowjo/downloads
GraphPad Prism 7.0	GraphPad Software	https://www.graphpad.com/scientific-software/prism/

CONTACT FOR REAGENT AND RESOURCE SHARING

Further information and requests for resources and reagents should be directed to and will be fulfilled by the Lead Contact, Dario S. Zamboni (dszamboni@fmrp.usp.br).

EXPERIMENTAL MODEL AND SUBJECT DETAILS

Animals

Mouse used in this study were in C57BL/6 genetic background and included C57BL/6 (Jackson Laboratory, stock number 000664), *Nlrp3*$^{-/-}$(Mariathasan et al., 2006), *Casp1/11*$^{-/-}$/*Casp11*^{Tg} (herein called *Casp1*$^{-/-}$) (Kayagaki et al., 2011), *Casp11*$^{-/-}$ (Kayagaki et al., 2011) and *Casp1/11*$^{-/-}$ (Kayagaki et al., 2011). Female mice ranging from six- to eight-weeks-old were bred and maintained under specific pathogen-free conditions at the University of São Paulo, FMRP/USP animal facility. All animals were provided food and water *ad libitum*, at 25°C. All experiments were conducted according to the guidelines from the institutional ethical committees for animal care from Comissão de ética em Experimentação Animal da Faculdade de Medicina de Ribeirão Preto, FMRP/USP, protocol number 14/2016.

Parasite culture and infection *in vivo*

Leishmania strains used were the following: *Leishmania (L.) amazonensis* PH8 strain (IFLA/BR/67/PH8), *Leishmania (L.) amazonensis* M2269 strain (MHOM/BR/73/M2269), which constitutively expresses GFP (*La-GFP*), *Leishmania (V.) braziliensis* M2903 strain (MHOM/BR/75/M2903), *Leishmania (L.) major* LV39 strain (MRHO/SU/59/P), *L. donovani* LD4 strain (MHOM/SD/00/1S-2D),*Leishmania (L.) major* LV39c5 *Lpg1*$^{-/-}$ mutant strain (M3P6), *Leishmania (L.) major* LV39c5 *Lpg1*$^{-/-}$/+*Lpg1* mutant strain (M3P4) and *Leishmania (L.) infantum* (HU-USF 8). *L. major* Lpg1$^{-/-}$ and *L. major Lpg1*$^{-/-}$/+*Lpg1* were kept in culture in the presence of Hygromycin B (15 μg mL^{-1}) and Puromycin (10 μg mL^{-1}), plus the addition of G418 (Geneticin) (10 μg mL^{-1}) for the later. Parasites were cultured at 25°C in Schneider's *Drosophila* medium (Invitrogen, Carlsbad, CA), pH 7.0, supplemented with 10% heat-inactivated fetal calf serum (GIBCO BRL), 100 U/ml penicillin G potassium (USB Corporation, Cleveland, OH, USA), 2 mM L-glutamine, and 2% human urine, pH 6.5. The infective-stage metacyclic promastigotes of *L. amazonensis* were isolated from stationary cultures through density gradient centrifugation, as described previously (Späth et al., 2003). For *in vivo* infections with *L. amazonensis,* mice were infected with either 1 × 10^6 stationary phase or 1 × 10^3 metacyclic promastigotes in 10 μL of PBS, through an intradermal injection into the left ear. Ear thicknesses were monitored weekly with a dial gauge caliper and compared to the thickness of the uninfected contralateral ear. Parasite burdens were determined in the ear and retromaxilar lymph node, which drains the site of infection.

METHOD DETAILS

Extraction and purification of LPG

Late log phase cells were harvested and washed twice with PBS prior to LPG extraction with solvent E (H_2O/ethanol/diethylether/ pyridine/ NH_4OH; 15:15:5:1:0.017). For purification, the solvent E extract was dried under N_2 evaporation, resuspendend in 2 mL of 0.1 N acetic acid/0.1 M NaCl, and subjected to hydrophobic chromatography using a column of phenyl-Sepharose. The column was sequentially washed with 6 mL of 0.1N acetic acid/0.1 M NaCl, 1 mL of 0.1 N acetic acid and 1 mL of endotoxin free water. The LPG was eluted with 4 mL of solvent E then dried under N_2 evaporation. LPG concentration was determined using the phenol-sulphuric method. All solutions were prepared in sterile, LPS-free distilled water (Sanobiol, Campinas, Brazil).

Bone marrow-derived macrophages and infection

Isolated femurs and tibia were flushed with incomplete RPMI, and the precursor cells were cultured in RPMI supplemented with 30% L929 cell-conditioned medium and 20% FBS. After 7 days in culture, the mature BMDMs were harvested and infected with stationary phase promastigotes at MOI 3, 5 or 10, depending on the *Leishmania* (indicated in figure legends). In killing experiments, free parasites were washed, and fresh media was added to the infected cultures after 1h of infection, and the parasite load was determined at 1, 48 and 96h post-infection via flow cytometric and *Giemsa* staining, using a FACS ACCURI C6 flow cytometer (BD Biosciences) and counting the Giemsa-stained cytospin preparations under a light microscope with a 100X objective, respectively. For flow cytometric analysis, cells were infected at different MOIs, and in the end of each time point, detached from the plate (without fixation) using trypsin, stained with LIVE/DEAD and analyzed. The flow cytometric data were analyzed using the FlowJo software (Tree Star). In this analysis, two parameters were considered: the percentage of infected cells and the integrated MFI (iMFI), which reflects the total functional response toward the infection and is calculated by the multiplication of the percentage of infected cells by the MFI. In *Giemsa* staining analysis, the infection rate was determined by scoring the % of infected macrophages (100 BMDMs counted) and the average number of intracellular parasites per cell.

Transfection experiments

Fully differentiated BMDMs were transfected with LPS (InvivoGen) (1 $\mu g\ mL^{-1}$) or highly purified LPGs from different *Leishmania* species. Cells were transfected with DOTAP Liposomal Transfection Reagent (Roche) or Lipofectamin 2000 reagent (Invitrogen) in RPMI (GIBCO) 1% FBS medium, according to manufacturer's instructions.

Cell death assay

Cells were transfected in phenol red-free RPMI medium for the indicated times, and then supernatants were collected and cell death was measured by the LDH release assay using the CytoTox 96 Non-Radioactive Cytotoxicity Assay kit (Promega). The values obtained are represented as percentage (%) compared to cell death induced by detergent lysis (3% Triton X-100).

Membrane pore formation assay

Kinetics of pore formation in BMDMs was quantified by the permeability to propidium iodide (PI) and its uptake by damaged cells. BMDMs were seeded in a black, clear-bottom 96-well plate, and before stimulation with LPG, BMDMs were washed with warm PBS, and the media were replenished with RPMI 10% FBS without phenol red, 0.038 g mL^{-1} NaHCO3, and 6 mg mL^{-1} PI. Infected BMDMs were kept at 37°C, and PI was excited at 538 nm. The fluorescence emission was read at 617 nm in 5 min intervals using a plate fluorometer (SpectraMax, Molecular Devices). The values obtained are represented as percentage (%) compared to cell death induced by detergent lysis (TritonX).

Endotoxin detection

The levels of endotoxin (LPS) were quantified by Limulus Amebocyte Lysate (LAL) assay kit (Lonza) in all highly pure LPG samples used in this study, according to manufacturer's instructions.

ROS detection

BMDMs were infected with stationary-phase promastigotes of *L. amazonensis* at an MOI of 10 or stimulated with PMA (200 ng/ml) for 90 min. Then, H2DCFDA (10 mM) was added to the cells for 30 min at 37°C. The cells were harvested and immediately analyzed by flow cytometry.

In vivo detection of CASP1

C57BL/6, *Nlrp3*$^{-/-}$ and *Casp11*$^{-/-}$ mice were injected with vehicle (PBS) or 10^6 *L. amazonensis* stationary-phase parasites. After 2 weeks of infection, the injected ears were removed, digested and macerated in collagenase. The macerate's supernatants were collected to measure CASP1 levels using CASP1 (mouse) ELISA KIT (Adipogen).

ELISA assay

The IL-1β, IL-1α and TNF-α production was assessed using IL-1β, IL-1α and TNF-α (BD Biosciences) ELISA KIT. CASP1 was measured using CASP1 (mouse) ELISA KIT (Adipogen). *In vitro* IL-1β production was analyzed in the cell-free supernatants harvested from the BMDMs pre-stimulated with 500 ng/ml of ultrapure LPS (InvivoGen), 10 ng/ml of TNF-α (eBioscience) or 300 ng/mL of PAM(3)CSK(4) (InvivoGen) for 4 hours and subsequently infected with stationary phase promastigotes at different MOI.

Endogenous CASP1 staining

The BMDMs were cultured and infected with stationary phase *Leishmania* at MOI 10. After 24 hours of infection, BMDMs were stained for 1 h with FAM–YVAD–fluoromethyl ketone (FAM–YVAD–FMK; Immunochemistry Technologies), as recommended by the manufacturer's instructions. The active CASP1 was then measured by flow cytometry. The data were acquired on a FACS ACCURI C6 flow cytometer (BD Biosciences) and analyzed with the FlowJo software (Tree Star).

Western blot

A total of 5×10^6 BMDMs were seeded per well, primed with ultrapure LPS (500 ng/ml) for 4 h and then infected with the different *Leishmania* species for 24 hours. The supernatants were collected and precipitated with 50% trichloroacetic acid and acetone. After their clarification by centrifugation, the cells were lysed in RIPA buffer (10 mM Tris-HCl, pH 7.4, 1 mM EDTA, 150 mM NaCl, 1% Nonidet P-40, 1% deoxycholate, and 0.1% SDS) containing protease inhibitor cocktail (Roche). The lysates and supernatants were resuspended in Laemmli buffer, boiled, resolved by SDS-PAGE and transferred (Semidry Transfer Cell, Bio-Rad) to a nitrocellulose membrane (GE Healthcare). The membranes were blocked in Tris-buffered saline (TBS) with 0.01% Tween-20 and 5% non-fat dry milk. The rat anti- CASP1 p20 monoclonal antibody clone 4B4 (Genentech) (1:500) and specific anti-rat horseradish peroxidase-conjugated antibodies (1:3000; KPL) were diluted in blocking buffer for the incubations. The ECL luminol reagent (GE Healthcare) was used for the antibody detection.

Casp4 activity assay

The Casp4 activity assay was performed as previously described (Shi et al., 2014). Briefly, each ligand was incubated with 0.15 μM of recombinant Casp4 protein, expressed in insect cells, in a buffer containing 50 mM HEPES (pH 7.5), 150 mM NaCl, 3 mM EDTA, 0.005% (v/v) Tween-20 and 10 mM DTT. After 30 min at 30°C, the Casp4 substrate Ac-WEHD-AFC was added into a reaction at a final concentration of 100 μM. The reaction mixtures were transferred to a 384-well plate and incubate at 37°C for another 30 min. Substrate cleavage was monitored by measuring the emission at 505 nm on excitation at 400 nm on a fluorescent multiwell reader (PerkinElmer Enpire Multimode Plate Reader).

Active CASP11 and LPG binding pull-down assay

For active CASP11 pull-down, primed BMDMs were replenished with fresh media containing 20 mM biotin-VAD-FMK (Enzo) 15 min before infection. Infected BMDMs were lysed in RIPA buffer (10mM Tris-HCl (pH 7.4), 1mM EDTA, 150mM NaCl, 1% Nonidet P-40, 1% (w/v) sodium deoxycholate and 0.1% (w/v) SDS) supplemented with protease inhibitor cocktail (Roche). Cleared lysates were equalized according to total protein content, incubated overnight with streptavidin-agarose beads (Invitrogen) and thoroughly rinsed with RIPA buffer. Bound proteins were eluted by re-suspension in Laemmli sample buffer, boiled for 5min and separated by SDS–polyacrylamide gel electrophoresis. LPG binding to CASP11 was performed as previously described for LPS binding (Shi et al., 2014). Briefly, Flag-tagged CASP11 was stable expressed in 293T cells and lysed in a buffer contaning 50 mM Tris-HCl (pH 7.6), 150 mM NaCl, 1% Triton X-100 and protease inhibitor cocktail. One μg of Biotin-conjugated LPS was first immobilized onto 10 μL of streptavidin Sepharose beads for each reaction. Cell lysate was pre-cleared with streptavidin Sepharose beads and 20 μg of unlabled LPS, LPG *L. braziliensis* or LPG *L. major* were incubated with pre-cleared lysates for 60 min at 4°C in constant rotation, and then biotinylated LPS-conjugated with streptavidin beads were added to the cell lysate for 90 min at 4°C. Beads were washed with lysis buffer for three times and boiled in 1X SDS sample loading buffer followed by Immunoblotting analyses.

Real-time PCR

Total RNA was extracted from 1×10^6 *Leishmania*-infected BMDMs (MOI 10) using TRIzol reagent (Invitrogen). Contaminating DNA was removed with an RNase-free DNase set (Promega). cDNA was synthesized from 1 μg of RNA using the SuperScript II reverse transcriptase (Invitrogen). Subsequent real-time PCR was performed on an AI PRISM 7000 sequence detector (Applied Biosystems) using SYBR Green (Invitrogen). The following primer sequences were used: *HPRT* forward (5′- TCAGTCAACGGGGGACATAAA-3′),

reverse (5′-AAGCCATGCCAATGTTGTCT-3′), *Tnfa* forward (5′-TGTGCTCAGAGCTTTCAACAA-3′), reverse (5′-CTTGATGGTGGTG CATGAGA-3′) and *Nos2* forward (5′-CGAAACGCTYCACTTCCAA-3′), reverse (5′- GGGGCTGTACTGCTTAACCAG −3′). The mRNA expression levels were normalized to HPRT. The adjusted values were calculated using the following formula: $2^{-(\text{CT target} - \text{CTHPRT})}$, where CT is the cycle threshold. The fold change in the expression was calculated as the *n*-fold difference in expression in the infected cells compared to the uninfected cells.

QUANTIFICATION AND STATISTICAL ANALYSIS

Statistical analysis

For the comparison of multiple groups, two-way analysis of variance (ANOVA), followed by the Bonferroni post-test were used. The differences in the values obtained for two different groups were determined using an unpaired, two-tailed Student's t test with a 95% confidence interval. Analyses were performed using the Prism 5.0 software (GraphPad, San Diego, CA). A difference was considered statistically significant when $p \leq 0.05$.